

Observation of viscous flux flow in $\text{YBa}_2\text{Cu}_3\text{O}_{7-\delta}$ low-angle grain boundaries

A. Díaz, L. Mechin,* P. Berghuis, and J. E. Evetts

Department of Materials Science and Metallurgy and IRC in Superconductivity, University of Cambridge, Pembroke Street, Cambridge CB2 3QZ, United Kingdom

(Received 8 April 1998)

The dynamics of vortices within an $\text{YBa}_2\text{Cu}_3\text{O}_{7-\delta}$ low-angle grain boundary have been investigated by means of current-voltage measurements with a magnetic field applied in the plane of the boundary. The high electric field regime can be explored without significant heating of the sample because the gauge length for the flux flow is of order the intervortex spacing, enabling the accurate determination of the flux flow resistivity ρ_f . It is observed that the well-known phenomenological expression $\rho_f/\rho_n \approx B/B_{c2}$ remains valid. The effect of the anisotropy of the superconductor on flux flow is also experimentally investigated. [S0163-1829(98)51130-7]

The motion of vortex lines under the Lorentz force arising from a current density \mathbf{j} , is an important topic that has been widely studied in the case of low-temperature superconductors (LTS). In particular, the viscous movement of vortices at currents sufficiently high as to overcome any pinning effects has been extensively investigated.¹⁻⁴ In this situation, the Lorentz force per unit length over a vortex line, $\mathbf{F}_L = \mathbf{j} \times \phi_0$ (ϕ_0 being the flux quantum), is balanced by the viscous drag and the dynamic pinning force. A moving vortex with a velocity \mathbf{v}_ϕ , experiences a viscous drag per unit length $\mathbf{F}_{\text{drag}} = \mathbf{v}_\phi \eta$, where η is the viscous drag coefficient. From pioneering experimental work by Kim, Hempstead, and Strnad⁵ a very simple relationship between the flux flow resistivity $\rho_f (= dE/dj)$ and the normal state resistivity ρ_n was established:

$$\rho_f/\rho_n \approx B/B_{c2}, \quad (1)$$

where $B = \mu_0 H$ is the magnetic flux density and $B_{c2} = \mu_0 H_{c2}$ with H_{c2} the upper critical field. Various models have explained this behavior by computing the viscosity η on fundamental grounds and under different constraints,^{6,7} the simplest one being the widely used Bardeen-Stephen model.⁷ Hao and Clem⁸ have extended this model for the case of anisotropic superconductors, arriving at similar expression to Eq. (1) along the different principal axes of the superconductor.

Experiments to investigate flux flow in high-temperature superconductors (HTS) by measuring the current-voltage (j - E) characteristics are particularly interesting. For example, B_{c2} may be determined provided the simple relation expressed by Eq. (1) is valid. However, such experiments are difficult to perform in HTS at high temperatures due to the dominance of thermally activated flux creep.⁹ These effects result in a highly nonlinear j - E response at low electric fields, moving the regime of viscous flux flow, where ρ_f can be safely determined, to high electric fields. Consequently, experimental care to avoid heating in the sample (current pulses, etc.) must be taken because of the high power density jE involved.^{10,11} Using pulsed current voltage measurements, Kunchur, Christen, and Philips¹⁰ have confirmed the validity of Eq. (1) for temperatures close to the critical tem-

perature T_c . Also, high frequency measurements, in which the vortices are oscillated within the pinning well potential, have been used to obtain η as well as the pinning parameters.¹² In what follows we demonstrate that $\text{YBa}_2\text{Cu}_3\text{O}_{7-\delta}$ (YBCO) low angle ($\leq 10^\circ$) [001]-tilt grain boundaries (GB) provide a useful model system whereby the viscous flux-flow regime can be accessed.

Recently we have established that a vortex state is reached in an YBCO low angle (4°) GB when the magnetic field \mathbf{H} is applied within the plane of the boundary.¹³ For \mathbf{H} perpendicular to the plane of the film (See Fig. 1), vortices are pinned in the boundary by the dislocation cores created to accommodate the bicrystal misorientation.^{13,14} If j ($\mathbf{j} \perp \mathbf{H}$) is in excess of the critical current density j_c , the narrow line of vortices pinned in the GB moves in response to the Lorentz force on the vortices, generating a voltage V across the boundary. It should be noted that this voltage is generated over a very short distance, of the order of a_0 (see below), around the boundary. As a consequence, even for very low voltages of a few μV , very high electric fields E of the order of 10^2 Vm^{-1} are generated. This electric field is around 10^4 times the usual field generated in a j - E measurement on an

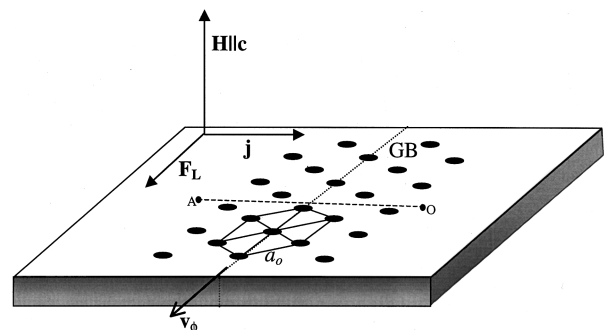


FIG. 1. Sketch of the hexagonal vortex lattice in the vicinity of a [001]-tilt grain boundary (GB). For an applied field \mathbf{H} within the plane of the GB, parallel to the c axis of the film, vortices are pinned by dislocation cores in the boundary. However, when a current in excess of the critical one is applied, vortices in the GB start to move with velocity \mathbf{v}_ϕ due to the Lorentz force \mathbf{F}_L directed along the GB.

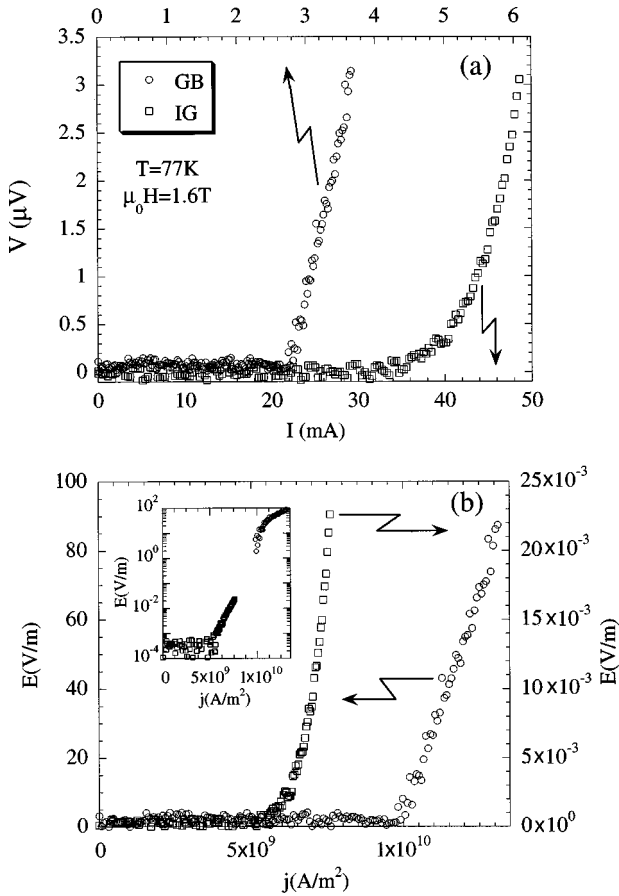


FIG. 2. (a) The measured current-voltage characteristics for both the grain boundary (GB) and the intragrain (IG). The IG curve has a pronounced rounding effect due to flux creep, however the GB trace is clearly linear, characteristic of simple flux flow. (b) The same curves as in (a) but normalized to yield the electric field E and current density j (see text for the calculation of j and E for the GB).

YBCO film track typically $100 \mu\text{m}$ long. Consequently high electric fields, well above the critical current region where flux creep dominates, can be achieved. Although the power density jE is very high (up to $1.5 \times 10^{12} \text{ Wm}^{-3}$ in our case), it is generated in a volume 10^4 times smaller than the track volume. Thus the *total* power dissipated is also 10^4 times smaller, leading to negligible heating of the sample.¹⁵ To verify these ideas we have made j - E measurements on both a 4° GB and the interior of the grain for an YBCO film deposited on a SrTiO_3 bicrystal. The film is the same used in a previous publication¹³ and experimental details are given there.

In Fig. 2(a) we present as measured current-voltage curves for the GB and for the interior of the grain (IG) at the same temperature and field (perpendicular to the plane of the film). Striking differences are apparent: in the IG curve typical rounding caused by flux creep can be observed, whereas the GB curve is highly linear. In Fig. 2(b) we have transformed the current-voltage data to j - E . In the case of the IG, as usual, we have just divided the measured voltage by the contact distance ($135 \mu\text{m}$) and the current by the track cross section ($0.16 \times 40 \mu\text{m}^2$). The calculation of j and E in the case of the GB requires a more careful analysis.

As discussed above, the voltage in the GB is generated by flow, with velocity v_ϕ , of the line of vortices in the bound-

ary (see Fig. 1). It is helpful to analyze the generation of the voltage induced by flux flow in terms of the Josephson relation^{1,2}

$$\partial\varphi_{AO}/\partial t = 2eV_{AO}/\hbar, \quad (2)$$

where φ_{AO} is the phase difference of the order parameter ψ between two points A and O at opposing sides of the junction, and V_{AO} is the instantaneous voltage generated by the changing phase. We assume that vortices on each side of the boundary remain pinned while a single row of vortices in the GB moves (see Fig. 1). Each vortex passing across the line connecting A and O induces a phase change 2π , and since the vortex spacing is a_0 ($a_0^2 = 2\phi_0/\sqrt{3}B$), the average rate of change of φ_{AO} , $\partial\varphi_{AO}/\partial t$, will be

$$\overline{\partial\varphi_{AO}/\partial t} = 2\pi\nu_\phi/a_0. \quad (3)$$

This can be inserted into Eq. (2) to yield \bar{V}_{AO} , the time averaged (i.e., measured) voltage between A and O :

$$\bar{V}_{AO} = \phi_0\nu_\phi/a_0. \quad (4)$$

Using the result $\bar{E}_{AO} = \nu_\phi B$ (Ref. 2) and combining with Eq. (4), we obtain

$$\bar{E}_{AO} = \bar{V}_{AO}Ba_0/\phi_0 = (2/\sqrt{3})\bar{V}_{AO}/a_0. \quad (5)$$

This result indicates that the effective length d_{eff} over which φ is changing is $d_{\text{eff}} = \sqrt{3}a_0/2$. We have therefore calculated the electric field E from the IV curves as $E = V/d_{\text{eff}} = 2V/\sqrt{3}a_0$. According to our assumption of a single row of vortices moving along the GB, while nearest neighbors at both sides of the GB remain pinned, this is fully self-consistent. Departures from this would change the value of E . For example, if a row two vortices wide moves (instead of one), d_{eff} is twice the value given here and hence E should be halved. However this implies a GB that is also $2a_0$ wide ($\approx 40 \text{ nm}$ at 7 T , the maximum field in our experiments) over the *whole* width of the track, otherwise the narrowest point should determine E according to Eq. (5). A common source of roughening of GB's is meandering, typically 50 nm for a high-angle GB.¹⁶ We have not found a corresponding value for a low-angle GB, although one expects a lower value since dislocations instead of overall crystalline disorder define the GB. The good numerical agreement found in this work using Eq. (5) strongly suggests that the effective length d_{eff} used is the proper one. The vortex movement in the GB resembles that of flux shear in artificial weak-pinning channel.¹⁷ However we note that in a GB there is strong pinning caused by the dislocations, also d_{eff} is determined by the intervortex distance and not by a constant channel width.

The calculation for the GB of j also requires discussion. It is well known that stresses associated with the dislocation cores in YBCO low-angle GB reduce the cross section of the current path.¹⁸ Therefore, it is convenient to introduce an effective cross section for current transport. A good estimate can be obtained by comparing j_c measurements on the GB and IG with \mathbf{H} parallel to the ab planes of the film.¹⁹ In this case no pinning by the GB dislocations should be observed and j_c should be similar for the IG and the GB track. Indeed we find that the ratio between the critical current densities of the IG and the GB tracks, $R_{j_c} = j_c(\text{IG}, H\parallel ab)/$

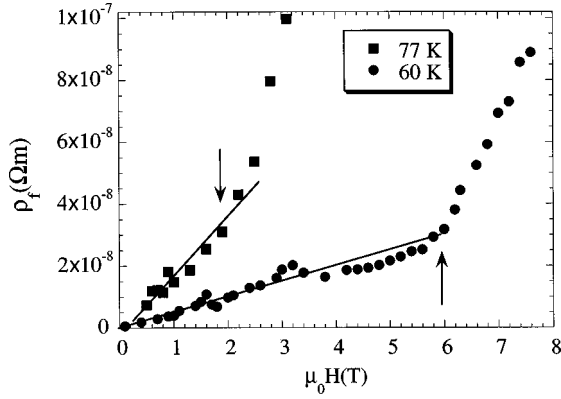


FIG. 3. Plot of the flux flow resistivity ρ_f versus the applied magnetic field at 60 K and 77 K for the GB. A linear part, in accordance with Kim's expression, Eq. (1), can be identified. The departure of ρ_f from this dependence occurs at a field B^* , marked with arrows in the figure.

$j_c(\text{GB}, H\parallel ab)$, is independent of field and temperature: $R_{j_c} = 4.3 \pm 0.6$. The difference between the IG and GB j_c is then assumed to arise from the reduction in the GB cross section caused by the dislocations cores which, obviously, does not depend on H and T . Moreover, the R_{j_c} value can be also deduced from the Chisholm and Pennycook model¹⁸ for a 4° ($\pm 0.5^\circ$) GB, for which the effective dislocation core has a diameter around 3.9 (± 0.7) nm leaving an undisturbed channel 1.7 (± 0.4) nm wide between the dislocations. As the distance D between dislocations is 5.6 ± 0.8 nm, one obtains $R_{j_c} = 3.5 \pm 0.5$. Therefore, we have determined a normalized j using an effective width $w_{\text{eff}} = w/4.3$ (where $w = 7.5$ μm is the nominal track width of the GB).

The result of these transformations can be seen in Fig. 2(b). The electric field range in the case of the GB is almost four order of magnitude larger than for the IG, well above the region where flux creep dominates. As a consequence, the GB j - E curve shows a clearly defined linear part above j_c which we interpret in terms of viscous flux flow. This part, as can be seen in the inset is, roughly, the prolongation of the curve corresponding to the IG. The good match between the two curves is an excellent validation of the procedure used to obtain E and j for the GB.

The next natural step is to investigate the validity of Eq. (1) for the GB. In Fig. 3 we present the values of ρ_f extracted from the j - E curves at different fields for two temperatures. A linear region where $\rho_f \propto B$ is clearly observed at the two temperatures, in agreement with Eq. (1), the two distinct slopes are due to the change in B_{c2} with temperature. We note that if a different normalization for E were chosen, for example, dividing V by a constant rather than a field dependent a_0 , a completely different dependence would be found, $\rho_f \propto B^{1/2}$, in disagreement with Eq. (1). This further supports the choice of a_0 as the gauge length for the electric field in a GB. Above a certain field B^* , ρ_f departs from the dependence $\propto B$, corresponding also to a rounding in the j - E curves. This happens at $B^* \approx 2$ T and $B^* \approx 6$ T at 77 K and 60 K respectively. One possible explanation for this is that, with increasing field (and interaction between vortices), some vortices at the banks of the boundary start to move and to contribute to E . This would increase the length d_{eff} over

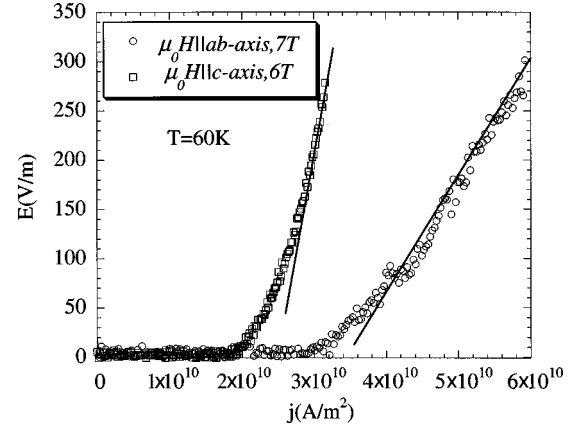


FIG. 4. j - E characteristics for the GB taken with the magnetic field applied perpendicular to the ab planes (squares) and parallel to the ab planes (circles) of the film. The different slopes are due to the anisotropy in the viscous flux flow of vortices moving either along the ab planes (squares) or crossing them (circles). Higher slope corresponds to higher flux flow resistivity.

which V is generated and, in turn, the values of E calculated by means of Eq. (5) would be increased relative to the actual value of E . However to clearly elucidate this point further work is necessary.

We may now calculate the values of B_{c2}^\perp (\perp meaning perpendicular to the ab planes) with the help of Eq. (1). First, from the linear part of the normal state resistivity ρ_n of our sample we get the value of the slope $d\rho_n/dT = 4.27 \times 10^{-9} \text{ } \Omega\text{m K}^{-1}$. As the residual resistivity $\rho_n(0)$ is negligible for these films, we obtain $\rho_n(77 \text{ K}) = 3.29 \times 10^{-7} \text{ } \Omega\text{m}$ and $\rho_n(60 \text{ K}) = 2.56 \times 10^{-7} \text{ } \Omega\text{m}$. Introducing these values into Eq. (1) together with the values of the slopes from the linear fits in Fig. (3), $d\rho_f/dB(77 \text{ K}) = 1.82 \times 10^{-8} \text{ } \Omega\text{m T}^{-1}$ and $d\rho_f/dB(60 \text{ K}) = 5.87 \times 10^{-9} \text{ } \Omega\text{m T}^{-1}$, we obtain $B_{c2}^\perp(77 \text{ K}) = 18.1 \text{ T}$ and $B_{c2}^\perp(60 \text{ K}) = 43.6 \text{ T}$. These results can be shown to be in very good agreement with the expected values at these temperatures. Thus from the Werthamer function²⁰ and $B_{c2}^\perp(0 \text{ K}) = 120 \text{ T}$,²¹ we obtain the values 17.7 T and 47.7 T for B_{c2}^\perp at 77 K and 60 K, respectively, in excellent agreement with our experimental values. Assuming a linear dependence of B_{c2} on T , $B_{c2}^\perp = (dB_{c2}^\perp/dT)(T_c - T)$ with $dB_{c2}^\perp/dT \approx 2 \text{ T/K}$ found experimentally by other authors,^{10,22} we deduce for our film (with $T_c = 87.3 \text{ K}$) $B_{c2}^\perp(77 \text{ K}) \approx 20.6 \text{ T}$ and $B_{c2}^\perp(60 \text{ K}) \approx 54.0 \text{ T}$. We note that the linear expression involved in this calculation has been used previously only for temperatures close to T_c , however the good numerical agreement found here for $T = 60 \text{ K}$ extends considerably its validity down to $T/T_c = 0.69$.

Values of the viscous drag coefficient η can also be calculated since $\eta = B_{c2} \phi_0 / \rho_n$ ($\phi_0 \approx 2.07 \times 10^{-15} \text{ Tm}^2$).¹ Using our experimental values from the previous paragraph we obtained $\eta(77 \text{ K}) = 1.1 \times 10^{-7} \text{ Nsm}^{-2}$ and $\eta(60 \text{ K}) = 3.4 \times 10^{-7} \text{ Nsm}^{-2}$. These estimates are in good agreement with values reported by other authors.¹²

Finally we have also measured ρ_f when \mathbf{H} is applied parallel to the ab planes but in the GB plane. Figure 4 shows a j - E curve taken at 60 K in this configuration together with one for which $H \perp ab$. Clearly the anisotropy has a pronounced effect on the j - E characteristic and the vortex vis-

cosity. Hao and Clem⁸ have analyzed the anisotropy of flux flow in HTS and give the ratio $\rho_c^{(a,b)}/\rho_{a,b}^{(c)} \approx 4/3\gamma$, where $\rho_i^{(k)}$ represents the flux flow resistivity for a vortex moving along the i axis when it lies along the k axis, and γ is the anisotropy parameter [$\gamma \approx 5-7$ for YBCO (Ref. 21)]. Accordingly, it is expected that, for the two configurations measured in Fig. 4, $\rho_c^{(a,b)}/\rho_{a,b}^{(c)} \approx 0.19-0.27$. From the fit in Fig. 4 the value $\rho_c^{(a,b)}(7\text{ T}) \approx 1.2 \times 10^{-8} \Omega\text{m}$ is obtained, and an extrapolation to $B=7\text{ T}$ of ρ_f in Fig. 3 gives the value $\rho_{a,b}^{(c)}(7\text{ T}) \approx 4.2 \times 10^{-8} \Omega\text{m}$. We therefore obtain an experimental value for $\rho_c^{(a,b)}/\rho_{a,b}^{(c)} \approx 0.29$, very close to the theoretical values predicted by the Hao and Clem model.

In conclusion, we have demonstrated that viscous flux flow dominates the flux dynamic response in an YBCO low-

angle GB even for very low voltage, due to the small size of the flux flow gauge length over which the phenomenon happens. The analysis of the flux flow resistivity shows that flux flow follows the well-known relation $\rho_f/\rho_n \approx B/B_{c2}$ as observed down to 60 K and below a field B^* . Also, the phenomenological model proposed by Hao and Clem for flux flow in layered superconductors has been tested. Due to its simplicity, the low-angle GB seems to provide an almost ideal system for experimental studies of vortex dynamics in HTS.

We would like to acknowledge support for this work from EPSRC. One of us (A.D.) wants to acknowledge support from the Spanish Ministerio de Educación y Cultura through a FPI post-doc grant.

*Present address: University of Twente, Faculty of Applied Physics, Low Temperature Division, P.O. Box 217, 7500 AE Enschede, The Netherlands.

¹M. Tinkham, *Introduction to Superconductivity*, 2nd edition (MacGraw-Hill, New York, 1996), Chap. 5.

²R. P. Huebener, *Magnetic Flux Structures in Superconductors* (Springer-Verlag, Berlin, 1979), Chap. 7.

³Y. B. Kim and M. J. Stephen, in *Superconductivity*, edited by R. D. Parks (Marcel Dekker, New York, 1969), Chap. 19.

⁴P. Berghuis and P. H. Kes, *Phys. Rev. B* **47**, 262 (1993).

⁵Y. B. Kim, C. F. Hempstead, and A. R. Strnad, *Phys. Rev. Lett.* **12**, 145 (1964); *Phys. Rev.* **139**, A1163 (1965).

⁶M. Tinkham, *Phys. Rev. Lett.* **13**, 804 (1964); J. R. Clem, *ibid.* **20**, 735 (1968); R. S. Thompson and C. R. Hu, *ibid.* **27**, 1352 (1971); *Phys. Rev. B* **6**, 110 (1972).

⁷J. Bardeen and M. J. Stephen, *Phys. Rev.* **140**, A1197 (1965).

⁸Z. Hao and J. R. Clem, *IEEE Trans. Magn.* **27**, 1086 (1991).

⁹For a review of vortices in HTS, see G. Blatter, M. V. Feigel'man, V. B. Geshkenbein, A. I. Larkin, and V. M. Vinokur, *Rev. Mod. Phys.* **66**, 1125 (1994).

¹⁰M. Kunchur, D. K. Christen, and J. M. Philips, *Phys. Rev. Lett.* **70**, 998 (1993).

¹¹S. Doettinger, R. P. Huebener, R. Gerdemann, A. Kühle, S. Anders, T. G. Träuble, and J. C. Villégier, *Phys. Rev. Lett.* **73**, 1691 (1994).

¹²See, for example, M. Golosovsky, M. Tsindlekht, and D. Davidov, *Supercond. Sci. Technol.* **9**, 1 (1996), and references therein.

¹³A. Díaz, L. Mechin, P. Berghuis, and J. E. Evetts, *Phys. Rev. Lett.* **80**, 3855 (1998).

¹⁴M. F. Chisholm and D. A. Smith, *Philos. Mag. A* **59**, 181 (1989).

¹⁵We have calculated, for our experimental conditions, the maximum increase in temperature in the sample ΔT to be below 8 mK when a power density $jE \approx 1.5 \times 10^{12} \text{ Wm}^{-3}$ is dissipated in the GB. For comparison, the same power density dissipated in the whole track gives $\Delta T \approx 19\text{ K}$.

¹⁶C. Træholt, J. G. Wen, H. W. Zandbergen, Y. Shen, and J. W. M. Hilgenkamp, *Physica C* **230**, 425 (1994).

¹⁷A. Pruyboom, P. H. Kes, E. van der Drift, and S. Radelaar, *Phys. Rev. Lett.* **60**, 1430 (1988).

¹⁸M. F. Chisholm and S. J. Pennycook, *Nature (London)* **351**, 47 (1991).

¹⁹We have calculated j_c using a $1\text{ }\mu\text{V}$ criterion. Note that the use of the same voltage criterion for both GB and IG leads to an error associated with the fact j_c is being estimated at different electric fields. Supposing the same $j-E$ behavior for the GB and IG, from Fig. 2(b) we can estimate a factor around 1.6 as an upper limit for the error. However, it is not clear that the GB $j-E$ curve must resemble the IG one at low E , and therefore we have preferred not to introduce a new unknown correction factor in the j_c calculation.

²⁰R. H. Werthamer, E. Helfand, and P. C. Hohenberg, *Phys. Rev.* **147**, 295 (1969).

²¹See, for example, T. Datta, in *Concise Encyclopedia of Magnetic and Superconducting Materials*, edited by J. E. Evetts (Pergamon, Oxford, 1992), p. 408.

²²U. Welp, W. K. Kwok, G. W. Crabtree, K. G. Vandervoort, and J. Z. Liu, *Phys. Rev. Lett.* **62**, 1908 (1989).